

This is a repository copy of *Sulfate production by reactive bromine: Implications for the global sulfur and reactive bromine budgets*.

White Rose Research Online URL for this paper:
<https://eprints.whiterose.ac.uk/119264/>

Version: Published Version

Article:

Chen, Q., Schmidt, J. A., Shah, V. et al. (3 more authors) (2017) Sulfate production by reactive bromine: Implications for the global sulfur and reactive bromine budgets. *Geophysical Research Letters*. GL073812. pp. 1-10. ISSN 1944-8007

<https://doi.org/10.1002/2017GL073812>

Reuse

Items deposited in White Rose Research Online are protected by copyright, with all rights reserved unless indicated otherwise. They may be downloaded and/or printed for private study, or other acts as permitted by national copyright laws. The publisher or other rights holders may allow further reproduction and re-use of the full text version. This is indicated by the licence information on the White Rose Research Online record for the item.

Takedown

If you consider content in White Rose Research Online to be in breach of UK law, please notify us by emailing eprints@whiterose.ac.uk including the URL of the record and the reason for the withdrawal request.

RESEARCH LETTER

10.1002/2017GL073812

Key Points:

- Inclusion of HOBr + S(IV) reactions in the model reduces global tropospheric Br_y burden by 50%
- Large fraction of sulfate is produced via HOBr oxidation in the presence of clouds and high HOBr abundance over low-latitude oceans
- In-cloud sulfate production via HOBr oxidation does not necessarily result in less gas-phase SO₂ oxidation

Supporting Information:

- Supporting Information S1

Correspondence to:

B. Alexander,
beckya@uw.edu

Citation:

Chen, Q., J. A. Schmidt, V. Shah, L. Jaeglé, T. Sherwen, and B. Alexander (2017), Sulfate production by reactive bromine: Implications for the global sulfur and reactive bromine budgets, *Geophys. Res. Lett.*, 44, doi:10.1002/2017GL073812.

Received 12 APR 2017

Accepted 23 JUN 2017

Accepted article online 27 JUN 2017

Sulfate production by reactive bromine: Implications for the global sulfur and reactive bromine budgets

Q. Chen¹ , J. A. Schmidt² , V. Shah¹ , L. Jaeglé¹ , T. Sherwen³ , and B. Alexander¹ 

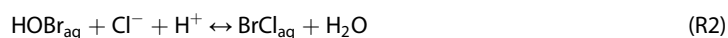
¹Department of Atmospheric Sciences, University of Washington, Seattle, Washington, USA, ²Department of Chemistry, University of Copenhagen, Copenhagen, Denmark, ³Wolfson Atmospheric Chemistry Laboratories, Department of Chemistry, University of York, York, UK

Abstract Sulfur and reactive bromine (Br_y) play important roles in tropospheric chemistry and the global radiation budget. The oxidation of dissolved SO₂ (S(IV)) by HOBr increases sulfate aerosol abundance and may also impact the Br_y budget, but is generally not included in global climate and chemistry models. In this study, we implement HOBr + S(IV) reactions into the Goddard Earth Observing System-Chem global chemical transport model and evaluate the global impacts on both sulfur and Br_y budgets. Modeled HOBr mixing ratios on the order of 0.1–1.0 parts per trillion (ppt) lead to HOBr + S(IV) contributing to 8% of global sulfate production and up to 45% over some tropical ocean regions with high HOBr mixing ratios (0.6–0.9 ppt). Inclusion of HOBr + S(IV) in the model leads to a global Br_y decrease of 50%, initiated by the decrease in bromide recycling in cloud droplets. Observations of HOBr are necessary to better understand the role of HOBr + S(IV) in tropospheric sulfur and Br_y cycles.

1. Introduction

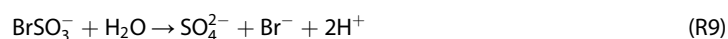
Reactive bromine (Br_y = BrO + Br + Br₂ + HOBr + BrCl + HBr + BrNO₃ + BrNO₂) has multiple impacts on tropospheric chemistry, including O₃ depletion, HO_x and NO_x perturbations, and oxidation of reduced sulfur species, volatile organic compounds (VOCs), and mercury [Vogt *et al.*, 1996; von Glasow *et al.*, 2004; Parrella *et al.*, 2012; Simpson *et al.*, 2015; Schmidt *et al.*, 2016]. The O₃ destruction driven by Br_y and the oxidation of SO₂ and VOCs by Br_y to produce sulfate and organic aerosols have implications for the radiative balance of the atmosphere and thus climate [von Glasow *et al.*, 2002; Saiz-Lopez *et al.*, 2012; Ofner *et al.*, 2012]. Box and 1-D modeling studies suggest that aqueous-phase oxidation of dissolved SO₂ (S(IV) = HSO₃⁻ + SO₃²⁻) by HOBr accounts for ~20% of sulfate production in the marine boundary layer (MBL) [Vogt *et al.*, 1996; von Glasow *et al.*, 2002]. This reaction is not included in global models of atmospheric chemistry due to uncertainties in reaction rates, which stem mainly from uncertainties in the abundance of HOBr [Chen *et al.*, 2016]. Recently, Chen *et al.* [2016] provided the first observational constraint on the importance of HOBr/HOCl + S(IV) for sulfate production in the remote, Southern Hemisphere MBL in spring and summer and found that hypohalous acids are responsible for 33–50% of sulfate formation. No studies have examined the implications of these reactions on the tropospheric Br_y budget.

The main sources of tropospheric Br_y are oxidation (by OH) and photolysis of bromocarbons (CH₃Br, CH₂Br₂, and CHBr₃) and sea salt aerosol (SSA) debromination [Parrella *et al.*, 2012; Carpenter *et al.*, 2014]. In polar regions, debromination has been proposed to occur on halide surface such as frost flowers [Rankin *et al.*, 2002], first-year sea ice [Simpson *et al.*, 2007a], blowing snow [Yang *et al.*, 2008], and snowpacks above tundra and first-year sea ice [Pratt *et al.*, 2013]. In addition, Br_y is transported from the stratosphere to the troposphere, but this source is minor globally [Schmidt *et al.*, 2016]. SSA debromination is thought to occur via uptake of HOBr followed by acid-catalyzed heterogeneous reaction with sea salt Br⁻ and Cl⁻ (R1)–(R6) [Fan and Jacob, 1992; Vogt *et al.*, 1996] to produce Br₂ (~90%) and BrCl (~10%) [Fickert *et al.*, 1999]. Br_y is mainly removed from the troposphere via wet and dry deposition to the Earth's surface and uptake by SSA to form Br⁻ [Schmidt *et al.*, 2016].





HOBr serves as one of the most abundant Br_y reservoirs in the troposphere during daytime, with modeled global tropospheric annual mean mixing ratio on the order of 0.1–1 parts per trillion (ppt = pmol/mol) [Fernandez *et al.*, 2014; Schmidt *et al.*, 2016]. Observations of HOBr abundance in the troposphere are sparse, with daytime concentrations ranging from 2 ppt (flight tracks over the tropical Western Pacific) [Le Breton *et al.*, 2017] to 10 ppt (surface observations in Alaska) [Liao *et al.*, 2012]. The effective Henry's law constant of HOBr (H_{HOBr}) is estimated to be between 93 and 6100 M atm⁻¹ [Sander, 2015; Chen *et al.*, 2016], so that >90% of HOBr is present in the gas phase even in the cloudy MBL. The small fraction of HOBr dissolved in aerosol or cloud liquid water reacts with Cl⁻ and Br⁻ to produce Br₂ and BrCl, rapidly recycling reactive bromine (R1)–(R6), and with S(IV) to produce sulfate (R7)–(R9) [Troy and Margerum, 1991; Liu, 2000].



In this study, we implement HOBr + S(IV) in Goddard Earth Observing System (GEOS)-Chem to investigate the effects of these reactions on both the sulfur and Br_y budgets.

2. GEOS-Chem Model

The model used in this study, GEOS-Chem v9-02, driven by GEOS-5 assimilated meteorological data from the NASA Goddard Earth Observing System, is a global three-dimensional chemical transport model (<http://www.geos-chem.org/>) of coupled aerosol-oxidant chemistry containing detailed HO_x-NO_x-VOC-ozone-BrO_x tropospheric chemistry [Schmidt *et al.*, 2016]. All simulations were performed at 4° × 5° horizontal resolution and 47 vertical levels up to 0.01 hPa. In order to compare the reactive bromine results presented in this study with those in Parrella *et al.* [2012] and Schmidt *et al.* [2016], we run all simulations for the year 2007, after spinning up the model for 1 year (2006). We run two main simulations: (i) without HOBr + S(IV) reactions, (ii) with HOBr + S(IV) reactions, and several sensitivity simulations by modifying sulfur emissions, SSA, and cloud properties to examine the effects of model uncertainties on the impacts of HOBr + S(IV) on tropospheric sulfur and Br_y budgets (Table S3 in the supporting information).

In the model, sulfate is produced via gas-phase oxidation of SO₂ by OH; in-cloud aqueous-phase oxidations of S(IV) by H₂O₂, O₃, and O₂ catalyzed by the transition metals iron and manganese [Park *et al.*, 2004; Alexander *et al.*, 2009, 2012]; and oxidation of S(IV) by O₃ on SSA [Alexander *et al.*, 2005]. The bulk cloud water pH is calculated as described in Alexander *et al.* [2012]. In this study, we have added in-cloud HOBr + S(IV) reactions to the model assuming first-order loss of HOBr via uptake by cloud droplets:

$$-\frac{d[\text{SO}_4^{2-}]}{dt} = \frac{d[\text{HOBr}]}{dt} = -\frac{c\gamma}{4} S[\text{HOBr}]$$

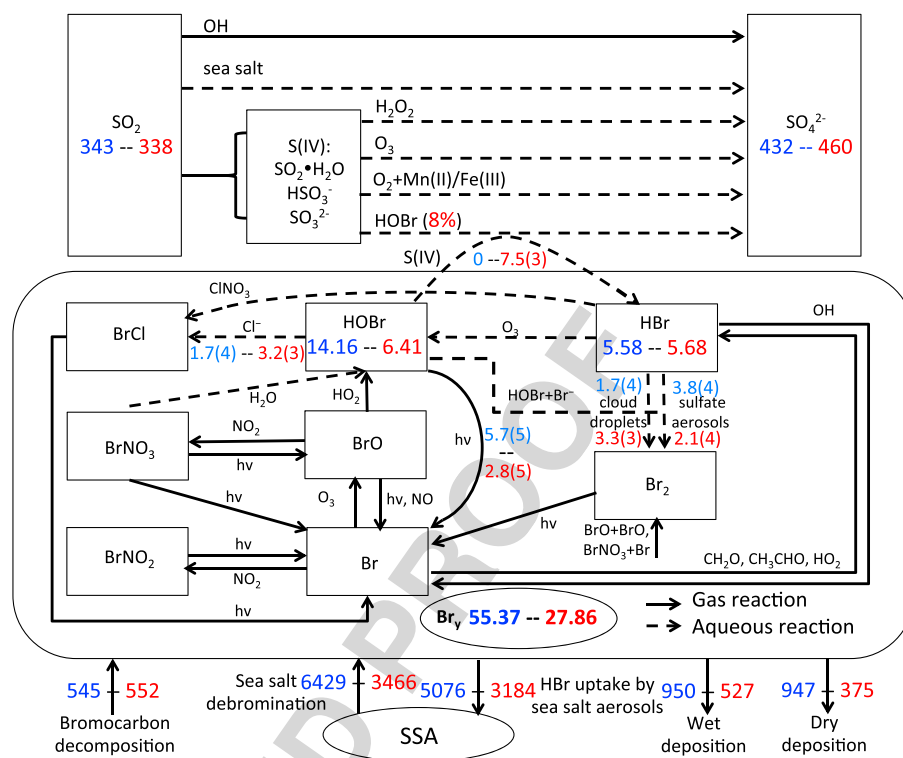


Figure 1. The global model budgets of tropospheric sulfur and Br_y for simulations without (blue color) and with (red color) HOBr + S(IV). Inventories (inside the boxes) are in units of Gg S for sulfur and Gg Br for Br_y. The solid arrows represent gas-phase reactions, while the dashed arrows represent aqueous-phase reactions. Production rates and loss rates of Br_y (below the big box) are in units of Gg Br a⁻¹. Loss rates for HOBr (next to the arrows) are in units of Gg Br a⁻¹. Read 7.5(3) as 7.5 × 10³. HOBr + S(IV) accounts for 8% of sulfate production.

where γ (unitless) is the reactive uptake coefficient of HOBr that involves gas diffusion, mass accommodation, and chemical reaction in the cloud droplets; c is the average thermal velocity of HOBr (unit: cm s⁻¹); S is the total surface area concentration of cloud droplets (unit: cm² cm⁻³). The reaction rate coefficient for the HOBr + HSO₃⁻ reaction ($k_{\text{HOBr}+\text{HSO}_3^-}$) and the HOBr + SO₃²⁻ reaction ($k_{\text{HOBr}+\text{SO}_3^{2-}}$) is 3.2 × 10⁹ M⁻¹ s⁻¹ [Liu, 2000] and 5.0 × 10⁹ M⁻¹ s⁻¹ [Troy and Margerum, 1991], respectively. More details about the implementation of HOBr + S(IV) in the model are shown in the supporting information. We neglect HOBr + S(IV) on SSA since most HOBr will react with Cl⁻ in SSA due to the much higher aqueous-phase concentration of Cl⁻ (SI).

We use the tropospheric bromine mechanism described by Schmidt *et al.* [2016]. SSA debromination via oxidation of Br⁻ by HOBr, O₃, and ClNO₃ on SSA was enabled as a sensitivity study in Schmidt *et al.* [2016] and is used in this study. There is no snow source of Br_y in the model.

3. Results and Discussion

3.1. Effects of HOBr + S(IV) Reactions on the Tropospheric Br_y Budget

Figure 1 shows the comparison of the tropospheric Br_y budgets between simulations with and without HOBr + S(IV). The modeled Br_y burden decreases by 50% after adding HOBr + S(IV) (additional sink of HOBr), initiated by the large (55%) decrease in HOBr abundance. The decrease in HOBr abundance in turn decreases SSA debromination, as more than 90% of SSA debromination occurred via reaction of HOBr with Br⁻ in sea salt aerosols (Br_{SSA}⁻) (R1)–(R6) before adding HOBr + S(IV) to the model. The global Br_y production rate from SSA debromination is 6429 Gg Br a⁻¹ and 3466 Gg Br a⁻¹ for simulations without and with HOBr + S(IV), respectively, with the latter magnitude closer to previous modeling estimates of 1150–2900 Gg Br a⁻¹ [Yang *et al.*, 2005; Parrella *et al.*, 2012; Fernandez *et al.*, 2014; Schmidt *et al.*, 2016]. Global

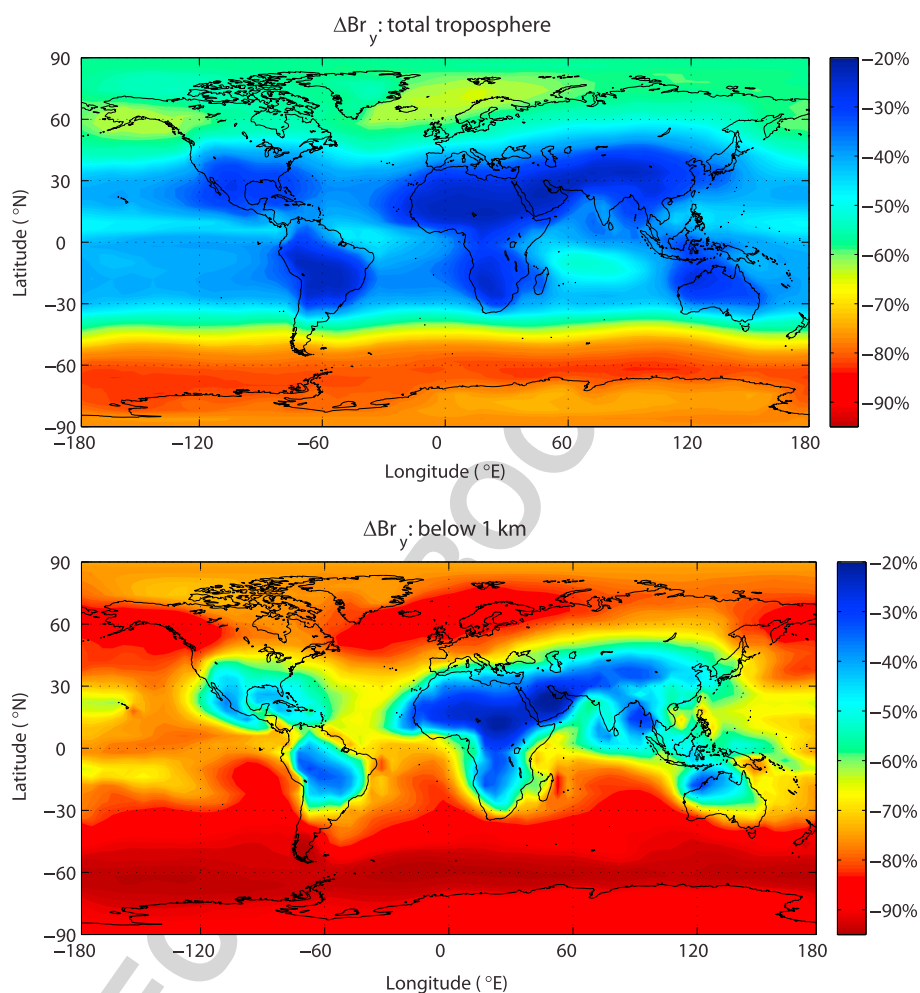


Figure 2. Percentage decrease in modeled annual mean Br_y burden in the (top) troposphere and (bottom) below 1 km after adding HOBr + S(IV).

bromocarbon decomposition rates are 545 Gg Br a^{-1} and 552 Gg Br a^{-1} for simulations without and with HOBr + S(IV), respectively, which is similar to recent global estimates ($520\text{--}550 \text{ Gg Br a}^{-1}$) [Parrella *et al.*, 2012; Schmidt *et al.*, 2016]. The small difference between the two simulations is due to higher OH concentrations in the model after adding HOBr + S(IV) due to lower Br_y , as discussed below. The decrease in HBr uptake by SSA, despite the slight increase in tropospheric burden of HBr, is because this process occurs mainly in the MBL where HBr abundance decreases (Figure S1 in the supporting information).

The addition of HOBr + S(IV) in the model lowers the burdens of all Br_y species, except HBr, by 28–75% (Table S1). The slight increase in HBr burden is due to the decrease in HBr removal by HOBr and the production of HBr (which is in equilibrium with Br^- in cloud droplets) from HOBr + S(IV) (R7)–(R9). HOBr + S(IV) competes with HOBr + Br^- in cloud droplets such that less HOBr is available for oxidizing Br^- to produce Br_2 . In our simulation with HOBr + S(IV), the amount of HOBr removed by reactions with S(IV) is 4.5 times that removed by reaction with Br^- in cloud droplets. This lowers the Br radical production rate, resulting in reductions in BrO and HOBr abundance. The lower HOBr abundance results in slower bromide recycling in both cloud droplets and sulfate aerosols. The lower HOBr abundance also results in even lower debromination from SSA, which is the largest source of Br_y in the lower troposphere. Previous studies have also shown that the bromine recycling on aerosols and cloud droplets (HOBr + Br^-) is critical for sustaining high Br_y levels in the troposphere [von Glasow *et al.*, 2004; Yang *et al.*, 2010; Parrella *et al.*, 2012; Schmidt *et al.*, 2016]. In particular, Parrella *et al.* [2012] reported a factor of 2 decrease in BrO mixing ratios when they turned off the HOBr + Br^- heterogeneous reaction in the model.

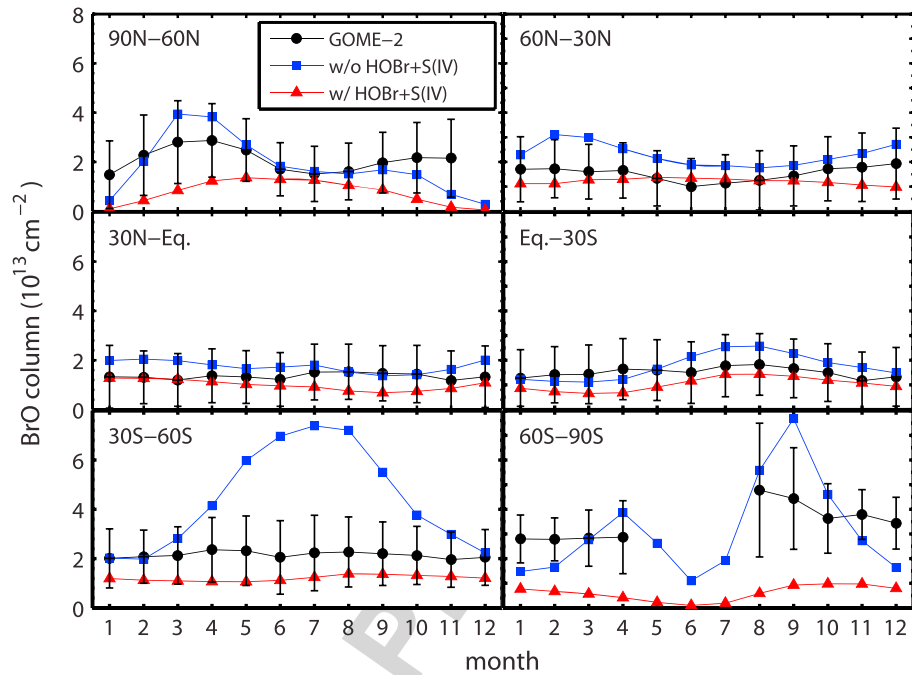


Figure 3. Comparison of modeled tropospheric BrO column with GOME-2 satellite observations of tropospheric BrO column (09:00–10:00) from *Theys et al.* [2011]. The error bars in the observations represent one standard deviation of spatial averaging.

Figure 2 shows the global annual mean distribution of percentage decreases in Br_y burden (ΔBr_y) in the total troposphere (Figure 2, top) and below 1 km (Figure 2, bottom) after adding HOBr + S(IV). The spatial pattern of the magnitude of the decrease in Br_y depends mainly on the amount of clouds for HOBr + S(IV) to occur and SSA abundance for debromination. In general, cloud fraction and cloud liquid water content (LWC) are high over the equator and high-latitude oceans such as Southern Ocean and low over the subtropics [*Molod et al.*, 2012; *Sud et al.*, 2013], while SSA burden is high over subtropics and high-latitude oceans and lower elsewhere [*Jaeglé et al.*, 2011]. Consequently, large decreases in Br_y occur over high-latitude oceans, especially Southern Ocean. A large decrease of Br_y over high-latitude oceans results in a large decrease of Br_y in polar regions from where Br_y is mainly transported. Note that there is no snow source of Br_y in the model. In the subtropics, Br_y is not as sensitive to HOBr + S(IV) because of low cloud amount, regardless of the high SSA abundance. In the lower troposphere (below 1 km), the decrease in Br_y is more significant, as HOBr + S(IV) mainly occur in the lower troposphere where clouds are present. The difference in ΔBr_y between low-latitude oceans and high-latitude oceans for the total troposphere is larger than that for MBL below 1 km, as upper troposphere Br_y reduction is smaller at low latitudes due to higher bromocarbon decomposition rates.

Figure 3 shows a comparison of modeled tropospheric BrO column with Global Ozone Monitoring Experiment (GOME)-2 satellite observations of tropospheric BrO column from *Theys et al.* [2011]. The addition of HOBr + S(IV) lowers modeled tropospheric BrO column globally throughout the year, with the impact increasing with increasing latitude. At low latitudes (30°S–30°N), the modeled BrO column is generally biased high for simulation without HOBr + S(IV) and biased low for the simulation with HOBr + S(IV), although both simulations are within the range of the observations. The addition of HOBr + S(IV) improves agreement with observations at midlatitudes (30°–60°). At high latitudes (60°–90°), the addition of HOBr + S(IV) causes the model to underestimate the observations by 60–80% (annual mean), where prior to adding HOBr + S(IV) the model underestimated the observations by only 7% at 90°–60°N and overestimated the observations by 2% at 60°S–90°S (annual mean). We expect the model to significantly underestimate observed BrO at high latitudes due to the lack of debromination in polar regions [*Simpson et al.*, 2007b]. We also note that the model does not include reactive iodine chemistry and includes very simple gas phase reactive chlorine

chemistry. Addition of reactive iodine and chlorine chemistry to the model will likely increase modeled BrO (and Br_y) abundances through Cl-Br-I interactions such as reactions of HOCl, HOI, ICl, and IBr with Br⁻ in aerosols and cloud droplets to sustain more efficient Br_y recycling [Vogt *et al.*, 1999; Ammann *et al.*, 2013; Sherwen *et al.*, 2016]. We expect this impact to be larger over midlatitude and high-latitude oceans where SSA abundance is high and clouds are frequent.

3.2. Effects of HOBr + S(IV) Reactions on the Tropospheric Sulfur Budget

Adding HOBr + S(IV) to the model increases both the global sulfate production rate and global sulfate burden by 6% (Figure 1). The global SO₂ burden decreases by only 2%, owing to the enhanced SO₂ production from oxidation of dimethyl sulfide (DMS) by OH. The global annual mean tropospheric OH concentration increases by 5% in the simulations with HOBr + S(IV) due to reductions in Br_y, resulting in an increase in the DMS oxidation rate by 6%. Vogt *et al.* [1996] suggested that oxidation of S(IV) by HOBr and HOCl on preexisting particles reduces the amount of SO₂ available for gas-phase oxidation and the formation of new cloud-condensation nuclei (CCN). The increase of OH abundance caused by reductions in Br_y after adding HOBr + S(IV) to the model, which was not considered in Vogt *et al.* [1996], could mitigate this CCN reduction effect via enhancing the SO₂ production rate from oxidation of DMS by OH. In our study, the change in the global sulfate production rate via the gas-phase reaction SO₂ + OH is negligible (<1%) after adding HOBr + S(IV) in the model.

For the model simulation with HOBr + S(IV), oxidation of S(IV) by HOBr accounts for 8% of sulfate production globally, mostly 96% via the HOBr+HSO₃⁻ channel as HSO₃⁻ is the dominant S(IV) species (>93%) in clouds at typical marine cloud pH between 3 and 6 [Faloona, 2009]. The corresponding tropospheric mean HOBr mixing ratio is about 0.4 ppt. In contrast, using the coupled chemistry-global climate model Community Atmosphere Model v4.6.33, Long *et al.* [2014] found that HOBr + S(IV) accounts for <1% of tropospheric sulfate formation globally (0.8% in clouds and 0.2% on SSA), despite similar HOBr mixing ratios (~0.3 ppt). A possible reason that Long *et al.* [2014] shows a small HOX + S(IV) contribution to sulfate formation could be that cloud chemistry is computed after gas phase chemistry in their model so that there is not a continuous supply of HOBr from the gas to the aqueous phase within the chemistry time step, as shown in their companion paper [Long *et al.*, 2013]. HOBr + S(IV) in cloud droplets in our study is coupled with gas phase chemistry, allowing for a continuous supply of HOBr produced from gas-phase reactions (e.g., BrO + HO₂). To confirm this explanation, we performed one sensitivity study in which HOBr + S(IV) in clouds was computed separately after gas phase chemistry and found that HOBr + S(IV) accounts for about 1% of sulfate formation globally, consistent with Long *et al.* [2014].

The percentage of sulfate produced from HOBr + S(IV) ($f_{\text{SO}_4\text{-HOBr}}$) varies from 0 to 45% (Figure 4a) in the lower troposphere, depending on a variety of factors including the abundance of different oxidants (mainly OH, H₂O₂, O₃, and HOBr), cloud fraction, cloud pH, and the concentrations of Cl⁻ and Br⁻ in cloud droplets that compete with HOBr + S(IV). In general, $f_{\text{SO}_4\text{-HOBr}}$ is smaller than 5% over the continents due to relatively low cloud fraction, high H₂O₂, and relatively low HOBr mixing ratios. Over the tropical oceans, $f_{\text{SO}_4\text{-HOBr}}$ reaches up to 45% where HOBr mixing ratios are high (Figure 4b). Higher HOBr mixing ratios do not guarantee higher $f_{\text{SO}_4\text{-HOBr}}$ however. Over the Arabian Sea west of India, the HOBr mixing ratio reaches about 0.8 ppt, but $f_{\text{SO}_4\text{-HOBr}}$ is only about 10% due to the limited amount of clouds. Over the South Atlantic Ocean west of Angola ([0°–20°S, 0°–20°E]), the HOBr mixing ratio reaches about 0.5 ppt, but $f_{\text{SO}_4\text{-HOBr}}$ is only about 15% due to relatively high H₂O₂ abundance.

Observations and calculations from Chen *et al.* [2016] suggested that 33–50% of sulfate in the Southern Hemisphere MBL during austral spring and summer (November–March) is produced via oxidation of S(IV) by HOBr and HOCl, suggesting daily mean HOBr + HOCl mixing ratio on the order of 0.01–0.1 ppt. In comparison, our model results show that only 7% of sulfate is produced via HOBr + S(IV) over the Southern Hemisphere MBL below 1 km during austral spring and summer, with a daily mean HOBr mixing ratio of 0.15 ppt. The difference in the calculated importance of S(IV) oxidation by hypohalous acids in these two studies, despite similar order-of-magnitude estimates of hypohalous acid abundance, is due to the fact that the gas-phase diffusion limitation of HOBr and HOCl was not considered in Chen *et al.* [2016] when calculating aqueous-phase production rates. Aqueous-phase reactions of HOBr with Cl⁻, Br⁻, and S(IV) are very rapid so that uptake of HOBr on the cloud droplets is limited by gas diffusion. Additionally, after HOBr enters the cloud droplets, Cl⁻ and Br⁻ remove HOBr and limit the availability of HOBr available for S(IV) oxidation.

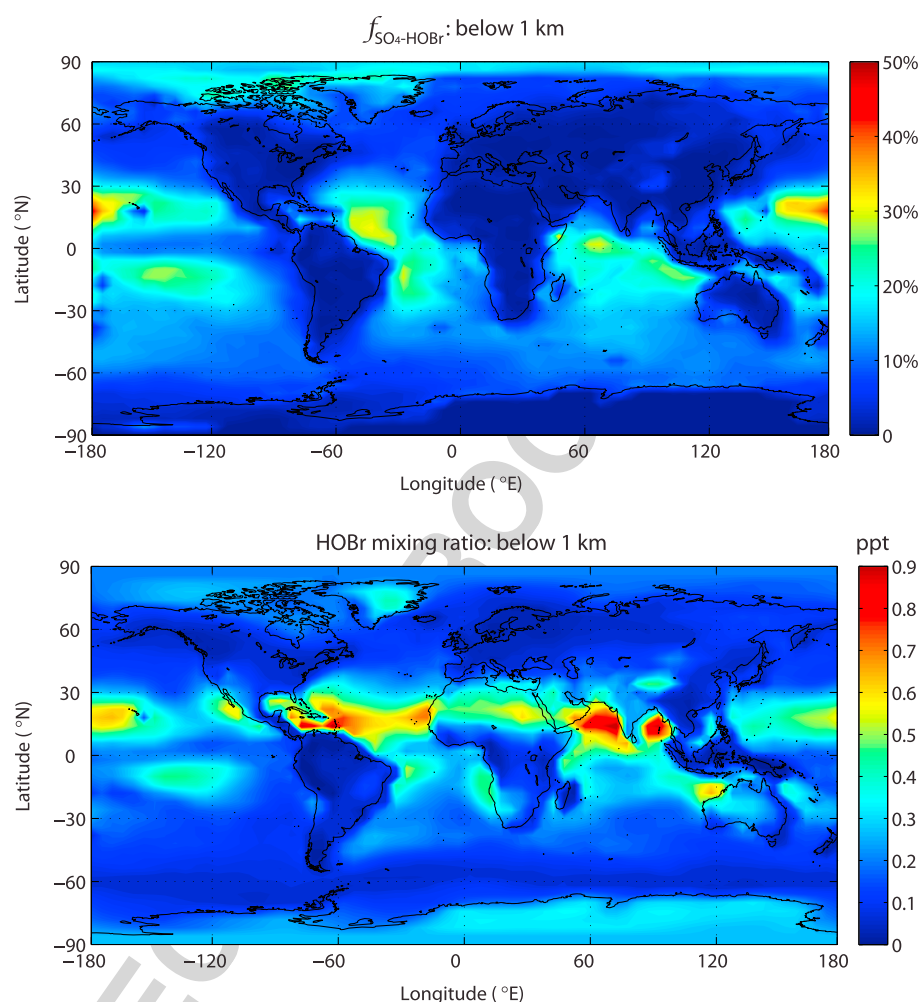


Figure 4. Global distribution of the percentage of annual mean sulfate produced via (top) HOBBr oxidation ($f_{\text{SO}_4\text{-HOBr}}$) and (bottom) HOBBr mixing ratio below 1 km for the model simulations with HOBr + S(IV).

The modeled underestimate of BrO (Figure 3), especially in the high southern latitudes, suggests that the modeled underestimate of the fraction of sulfate produced from HOBr and HOCl is due to a modeled low bias in HOBr, in addition to the lack of S(IV) oxidation by HOCl in the model.

4. Implications

The large impacts of HOBr + S(IV) on the reactive bromine budget in the model have further implications for the oxidation capacity of the atmosphere via its impacts on the burden of O_3 and the partitioning of HO_x ($\text{OH} + \text{HO}_2$) and NO_x ($\text{NO} + \text{NO}_2$) [von Glasow *et al.*, 2004]. Reactive bromine destroys O_3 through the Br-BrO cycle. A 50% reduction of Br_y burden after adding HOBr + S(IV) results in a 5 ppb increase in global mean tropospheric O_3 (up to 10 ppb over Southern Ocean and Antarctica). Reactive bromine perturbs HO_x partitioning via $\text{BrO} + \text{HO}_2$ to produce HOBr and subsequent photolysis of HOBr to produce Br and OH. Based on this, a reduction of Br_y burden after adding HOBr + S(IV) should result in a decrease in OH. However, this effect is compensated by the increase in O_3 . As such, tropospheric OH abundance increases by 5% after adding HOBr + S(IV). This is consistent with the previous finding that the impact of Br_y on OH occurs mainly via the O_3 destruction channel rather than the HO_2 conversion by BrO channel [Parrella *et al.*, 2012; Wang *et al.*, 2015]. Reactive bromine removes NO_x via $\text{BrO} + \text{NO}_2$ to produce BrNO_3 and subsequent hydrolysis of BrNO_3 to produce nitrate. After adding HOBr + S(IV), tropospheric NO_x burden

increases by 3% globally, up to 90% over Southern Ocean, although the absolute abundance of NO_x is very low in this region (several parts per trillion).

The important role of $\text{HOBr} + \text{S(IV)}$ on the Br_y budget suggests that changes in sulfur emissions could impact the oxidative capacity of the troposphere. We conduct two sensitivity studies using our model simulations with $\text{HOBr} + \text{S(IV)}$ to examine potential impacts of changes in sulfur emissions on Br_y and oxidant budgets. First, we examine the impacts of anthropogenic emissions of sulfur by switching off anthropogenic sulfur emissions in the model, which reduces the total emissions of sulfur ($\text{SO}_2 + \text{DMS}$) by 73%. The change in the Br_y burden is less than 1% globally, with regional increases up to 5% over China and regional decrease up to 4% over the north Indian Ocean. The change in tropospheric O_3 mixing ratio is less than 1.1 ppb everywhere. The small change in Br_y and oxidant budgets when turning off anthropogenic sulfur emissions is due to the fact that most anthropogenic emissions occur over continents where HOBr is relatively low and clouds are few, and because the resulting increase in cloud pH due to a reduction in SO_2 emissions slows down the acid-catalyzed $\text{HOBr} + \text{Br}^-$ reaction in cloud droplets. In a second sensitivity simulation, we examine the impact of changing sulfur emissions on tropospheric Br_y and oxidant budgets during preindustrial times by doubling DMS emission together with turning off anthropogenic sulfur emissions in the model. The change in Br_y burden is also less than 1% globally, with regional increases up to 3% over Southern Ocean where pH decreases by 0.4 and regional decrease up to 2% over some Northern Hemisphere ocean regions where pH decreases by less than 0.2. Thus, changes in sulfur emissions have a small impact on the global Br_y budget due to compensating effects of changes in the sink of HOBr (via $\text{HOBr} + \text{S(IV)}$) and changes in the acid-catalyzed production rate of Br_y (R1)–(R6). This emphasizes the importance of explicitly considering changes in cloud pH when evaluating potential impacts on changing emissions on the global Br_y budget. It should be noted from Figure 1 that a change in cloud pH after adding $\text{HOBr} + \text{S(IV)}$ in the model is negligible in this study as the sulfate burden change is only 6%.

Other sensitivity scenarios (Table S3) examining the importance of model uncertainties on the impacts of $\text{HOBr} + \text{S(IV)}$ include doubling SSA emission, doubling SSA bromide concentrations ($[\text{Br}_{\text{SSA}}^-]$), reducing coarse-mode SSA pH by two units, reducing $k_{\text{HOBr}+\text{HSO}_3^-}$ by 2 orders of magnitude, doubling cloud LWC, reducing cloud pH by one unit, and increasing both $[\text{Cl}^-]$ and $[\text{Br}^-]$ concentrations in clouds by 1 order of magnitude. For all these scenarios, the percentage increase in annual mean tropospheric sulfate burden (ΔSO_4) varies from 6% to 8%, the percentage decrease in Br_y (ΔBr_y) varies from -42% to -57% , and the fraction of sulfate abundance formed from $\text{HOBr} + \text{S(IV)}$ ($f_{\text{SO}_4\text{-HOBr}}$) varies from 7% to 11% after adding $\text{HOBr} + \text{S(IV)}$, which do not differ significantly from the standard model runs ($\Delta\text{SO}_4 = 6\%$; $\Delta\text{Br}_y = -50\%$; $f_{\text{SO}_4\text{-HOBr}} = 8\%$). Doubling SSA emissions does not result in a doubling of Br_y abundance (only 18–38% increase) because SSA also provides a surface for uptake of HBr , which partially compensates for the increased SSA emissions flux by reducing the lifetime of HBr . Additionally, SSA is not the only source of Br_y in the troposphere. Doubling $[\text{Br}_{\text{SSA}}^-]$ and reducing coarse-mode SSA pH by two units do not result in significant changes in tropospheric Br_y burden ($<5\%$) because the uptake of HOBr by SSA is limited by gas phase diffusion of HOBr in the MBL (SI). $f_{\text{SO}_4\text{-HOBr}}$ remains small (8%–9%) when doubling $[\text{Br}_{\text{SSA}}^-]$ and reducing coarse-mode SSA pH because of the small changes in Br_y abundance. Tropospheric sulfate and Br_y burdens are not very sensitive to the changes in $k_{\text{HOBr}+\text{HSO}_3^-}$ (and H_{HOBr}), cloud LWC, cloud pH, and Cl^- and Br^- concentrations in cloud droplets because uptake of HOBr by cloud droplets is limited by gas diffusion of HOBr and $\text{HOBr} + \text{S(IV)}$ is much faster (up to 5 orders of magnitude) than $\text{HOBr} + \text{Cl}^-/\text{Br}^-$ in cloud droplets (SI). In sum, the impact of adding $\text{HOBr} + \text{S(IV)}$ to the model is not highly sensitive to the varied model parameters. We note that missing processes in the model such as interactions with reactive iodine or Br_y sources in polar regions could significantly impact Br_y abundance and $f_{\text{SO}_4\text{-HOBr}}$.

5. Conclusions

It has been proposed that hypohalous acids such as HOBr could be responsible for a large fraction of sulfate production in the MBL [Vogt *et al.*, 1996; von Glasow *et al.*, 2002; Chen *et al.*, 2016]. Here we implemented $\text{HOBr} + \text{S(IV)}$ reactions into GEOS-Chem for the first time to investigate the global impact of these reactions on both tropospheric sulfur and reactive bromine budgets. Adding $\text{HOBr} + \text{S(IV)}$ increased the global sulfate production rate by 6% and decreased the global Br_y burden by 50%. About 8% of sulfate is produced via

HOBr oxidation globally, under a global mean HOBr mixing ratio of 0.4 ppt. The reduction in Br_y resulting from adding HOBr + S(IV) to the model led to an increase in O₃, OH, and NO_x abundances. Increases in OH resulted in an increased production rate of SO₂ from DMS + OH, compensating for reductions in SO₂ from faster removal by HOBr + S(IV), leading to negligible change in the gas-phase sulfate production rate from SO₂ + OH. Changes in sulfur emissions after adding HOBr + S(IV) did not significantly impact the global Br_y and oxidant budgets on the global scale because of compensating effects of cloud pH on acid-catalyzed reactive bromine production. This study, combined with our previous study on Δ¹⁷O of sulfate in the MBL [Chen *et al.*, 2016], suggests that reactive halogens could play an important role in sulfate production in the MBL, even with HOBr mixing ratios as low as sub-ppt levels. Due to the large impacts of HOBr + S(IV) reactions on tropospheric sulfur and reactive bromine budgets, we recommend including HOBr + S(IV) reactions in global models of tropospheric chemistry and climate and prioritizing observations of tropospheric HOBr abundance.

Acknowledgments

We acknowledge NSF AGS award 1343077 to B.A. for support of this research. J.A.S. acknowledges support from the Calsberg Foundation (CF19-0519). The data used are listed in the references, figures, and supporting information.

References

- Alexander, B., R. J. Park, D. J. Jacob, Q. B. Li, R. M. Yantosca, J. Savarino, C. C. W. Lee, and M. H. Thieme (2005), Sulfate formation in sea-salt aerosols: Constraints from oxygen isotopes, *J. Geophys. Res.*, *110*, D10307, doi:10.1029/2004JD005659.
- Alexander, B., R. J. Park, D. J. Jacob, and S. Gong (2009), Transition metal catalyzed oxidation of atmospheric sulfur: Global implications for the sulfur budget, *J. Geophys. Res.*, *114*, D02309, doi:10.1029/2008JD010486.
- Alexander, B., D. J. Allman, H. M. Amos, T. D. Fairlie, J. Dachs, D. A. Hegg, and R. S. Sletten (2012), Isotopic constraints on the formation pathways of sulfate aerosol in the marine boundary layer of the subtropical northeast Atlantic Ocean, *J. Geophys. Res.*, *117*, D06304, doi:10.1029/2011JD016773.
- Ammann, M., R. A. Cox, J. N. Crowley, M. E. Jenkin, A. Mellouki, M. J. Rossi, J. Troe, and T. J. Wallington (2013), Evaluated kinetic and photochemical data for atmospheric chemistry: Volume vi heterogeneous reactions with liquid substrates, *Atmos. Chem. Phys.*, *13*, 8045–8228, doi:10.5194/acp-13-8045-2013.
- Beckwith, R. C., T. X. Wang, and D. W. Margerum (1996), Equilibrium and kinetics of bromine hydrolysis, *Inorg. Chem.*, *35*, 995–1000.
- Carpenter, L. J. and S. Reimann (Lead Authors), J. B. Burkholder, C. Clerbaux, B. D. Hall, R. Hossaini, J. C. Laube, and S. A. Yvon-Lewis (2014), Ozone-depleting substances (ODSs) and other gases of interest to the Montreal protocol, Chapter 1 in Scientific Assessment of Ozone Depletion: 2014, Global Ozone Research and Monitoring Project – Report No. 55, World Meteorological Organization, Geneva, Switzerland.
- Chen, Q., L. Geng, J. A. Schmidt, Z. Xie, H. Kang, J. Dachs, J. Cole-Dai, A. J. Schauer, M. G. Camp, and B. Alexander (2016), Isotopic constraints on the role of hypohalous acids in sulfate aerosol formation in the remote marine boundary layer, *Atmos. Chem. Phys.*, *16*, 11,433–11,450, doi:10.5194/acp-16-11433-2016.
- Faloona, I. (2009), Sulfur processing in the marine atmospheric boundary layer: A review and critical assessment of modeling uncertainties, *Atmos. Environ.*, *43*, 2841–2854, doi:10.1016/j.atmosenv.2009.02.043.
- Fan, S.-M. and D. J. Jacob (1992), Surface ozone depletion in Arctic spring sustained by bromine reactions on aerosols, *Nature*, *359*, 522–524, doi:10.1038/359522a0.
- Fernandez, R. P., R. J. Salawitch, D. E. Kinnison, J.-F. Lamarque, and A. Saiz-Lopez (2014), Bromine partitioning in the tropical tropopause layer: Implications for stratospheric injection, *Atmos. Chem. Phys.*, *14*(24), 13,391–13,410, doi:10.5194/acp-14-13391-2014.
- Fickert, S., J. W. Adams, and J. N. Crowley (1999), Activation of Br₂ and BrCl via uptake of HOBr onto aqueous salt solutions, *J. Geophys. Res.*, *104*(D19), 23,719–23,727, doi:10.1029/1999JD900359.
- Jaeglé, L., P. K. Quinn, T. S. Bates, B. Alexander, and J.-T. Lin (2011), Global distribution of sea salt aerosols: New constraints from in situ and remote sensing observations, *Atmos. Chem. Phys.*, *11*, 3137–3157, doi:10.5194/acp-11-3137-2011.
- Le Breton, M., et al. (2017), Enhanced ozone loss by active inorganic bromine chemistry in the tropical troposphere, *Atmos. Environ.*, *155*, 21–28, doi:10.1016/j.atmosenv.2017.02.003.
- Liao, J., et al. (2012), Observations of inorganic bromine (HOBr, BrO, and Br₂) speciation at Barrow, Alaska, in spring 2009, *J. Geophys. Res.*, *117*, D00R16, doi:10.1029/2011JD016641.
- Liu, Q. (2000), Kinetics of aqueous phase reactions related to ozone depletion in the arctic troposphere: Bromine chloride hydrolysis, bromide ion with ozone, and sulfur(IV) with bromine and hypobromous acid, Ph.D. thesis, Department of Chemistry, Purdue University, USA, 253 pp.
- Liu, Q. and D. W. Margerum (2001), Equilibrium and kinetics of bromine chloride hydrolysis, *Environ. Sci. Technol.*, *35*, 1127–1133.
- Long, M. S., W. C. Keene, R. Easter, R. Sander, A. Kerkweg, D. Erickson, X. Liu, and S. Ghan (2013), Implementation of the chemistry module MECCA (v2.5) in the modal aerosol version of the Community Atmosphere Model component (v3.6.33) of the Community Earth System Model, *Geosci. Model Dev.*, *6*, 255–262, doi:10.5194/gmd-6-255-2013.
- Long, M. S., W. C. Keene, R. C. Easter, R. Sander, X. Liu, A. Kerkweg, and D. Erickson (2014), Sensitivity of tropospheric chemical composition to halogen-radical chemistry using a fully coupled size-resolved multiphase chemistry–global climate system: Halogen distributions, aerosol composition, and sensitivity of climate-relevant gases, *Atmos. Chem. Phys.*, *14*, 3397–3425, doi:10.5194/acp-14-3397-2014.
- Molod, A., L. Takacs, M. J. Suarez, J. Bacmeister, I.-S. Song, and A. Eichmann (2012), GEOS-5 atmospheric general circulation model: Mean climate development from MERRA to Fortuna, Tech. Memo., NASA Goddard Space Flight Center, MD, 115 pp.
- Ofner, J., N. Balzer, J. Buxmann, H. Grothe, Ph. Schmitt-Kopplin, U. Platt, and C. Zetzsch (2012), Halogenation processes of secondary organic aerosol and implications on halogen release mechanisms, *Atmos. Chem. Phys.*, *12*, 5787–5806, doi:10.5194/acp-12-5787-2012.
- Park, R. J., D. J. Jacob, B. D. Field, R. M. Yantosca, and M. Chin (2004), Natural and transboundary pollution influences on sulfate-nitrate-ammonium aerosols in the United States: Implications for policy, *J. Geophys. Res.*, *109*, D15204, doi:10.1029/2003JD004473.
- Parrella, J. P., D. J. Jacob, Q. Liang, Y. Zhang, L. J. Mickley, B. Miller, M. J. Evans, X. Yang, J. A. Pyle, N. Theys, and M. Van Roozendael (2012), Tropospheric bromine chemistry: Implications for present and pre-industrial ozone and mercury, *Atmos. Chem. Phys.*, *12*, 6723–6740, doi:10.5194/acp-12-6723-2012.
- Pratt, K. A., et al. (2013), Photochemical production of molecular bromine in Arctic surface snowpacks, *Nature Geosci.*, *6*, 351–356.

- Rankin, A. M., E. W. Wolff, and S. Martin (2002), Frost flowers: Implications for tropospheric chemistry and ice core interpretation, *J. Geophys. Res.*, *107*(D23), 4683, doi:10.1029/2002JD002492.
- Saiz-Lopez, A., et al. (2012), Estimating the climate significance of halogen-driven ozone loss in the tropical marine troposphere, *Atmos. Chem. Phys.*, *12*, 3939–3949, doi:10.5194/acp-12-3939-2012.
- Sander, R. (2015), Compilation of Henry's law constants (version 4.0) for water as solvent, *Atmos. Chem. Phys.*, *15*, 4399–4981, doi:10.5194/acp-15-4399-2015.
- Schmidt, J. A., et al. (2016), Modeling the observed tropospheric BrO background: Importance of multiphase chemistry and implications for ozone, OH, and mercury, *J. Geophys. Res.-Atmos.*, *121*, 155–157, doi:10.1002/2015JD024229.
- Sherwen, T., et al. (2016), Global impacts of tropospheric halogens (Cl, Br, I) on oxidants and composition in GEOS-Chem, *Atmos. Chem. Phys.*, *16*, 12239–12271, doi:10.5194/acp-16-12239-2016.
- Simpson, W. R., D. Carlson, G. Hönninger, T. A. Douglas, M. Sturm, D. Perovich, and U. Platt (2007a), First-year sea-ice contact predicts bromine monoxide (BrO) levels at Barrow, Alaska better than potential frost flower contact, *Atmos. Chem. Phys.*, *7*, 621–627, doi:10.5194/acp-7-621-2007.
- Simpson, W. R., et al. (2007b), Halogens and their role in polar boundary-layer ozone depletion, *Atmos. Chem. Phys.*, *7*, 4375–4418, doi:10.5194/acp-7-4375-2007.
- Simpson, W. R., S. S. Brown, A. Saiz-Lopez, J. A. Thornton and R. von Glasow (2015), Tropospheric halogen chemistry: Sources, cycling, and impacts, *Chem. Rev.*, *115*, 4035–4062, doi:10.1021/cr5006638.
- Sud, Y. C., D. Lee, L. Oreopoulos, D. Barahona, A. Nees, and M. J. Suarez (2013), Performance of McRAS-AC in the GEOS-5 AGCM: Aerosol-cloud-microphysics, precipitation, cloud radiative effects, and circulation, *Geosci. Model Dev.*, *6*, 57e79, doi:10.5194/gmd-6-57-2013.
- Theys, N., M. Van Roozendael, F. Hendrick, X. Yang, I. De Smedt, A. Richter, M. Begoin, Q. Errera, P. V. Johnston, K. Kreher, and M. De Mazière (2011), Global observations of tropospheric BrO columns using GOME-2 satellite data, *Atmos. Chem. Phys.*, *11*, 1791–1811, doi:10.5194/acp-11-1791-2011.
- Troy, R. C., and D. W. Margerum (1991), Non-metal redox kinetics: Hypobromite and hypobromous acid reactions with iodide and with sulfite and the hydrolysis of bromosulfate, *Inorg. Chem.*, *30*, 3538–3543, doi:10.1021/ic00018a028.
- Vogt, R., P. J. Crutzen, and R. Sander (1996), A mechanism for halogen release from sea-salt aerosol in the remote marine boundary layer, *Nature*, *383*, 327–330, doi:10.1038/383327a0.
- Vogt, R., R. Sander, R. von Glasow, and P. J. Crutzen (1999), Iodine chemistry and its role in halogen activation and ozone loss in the marine boundary layer: A model study, *J. Atmos. Chem.*, *32*, 375–395.
- von Glasow, R., R. Sander, A. Bott, and P. J. Crutzen (2002), Modeling halogen chemistry in the marine boundary layer. 2. Interactions with sulfur and the cloud-covered MBL, *J. Geophys. Res.*, *107*(D17), 4323, doi:10.1029/2001JD000943.
- von Glasow, R., R. von Kuhlmann, M. G. Lawrence, U. Platt, and P. J. Crutzen (2004), Impact of reactive bromine chemistry in the troposphere, *Atmos. Chem. Phys.*, *4*, 2481–2497, doi:10.5194/acp-4-2481-2004.
- Wang, S., et al. (2015), Active and widespread halogen chemistry in the tropical and subtropical free troposphere, *Proc. Natl. Acad. Sci. U.S.A.*, *112*, 9281–9286, doi:10.1073/pnas.1505142112.
- Yang, X., R. A. Cox, N. J. Warwick, J. A. Pyle, G. D. Carver, F. M. O'Connor, and N. H. Savage (2005), Tropospheric bromine chemistry and its impacts on ozone: A model study, *J. Geophys. Res.*, *110*, D23311, doi:10.1029/2005JD006244.
- Yang, X., J. A. Pyle, and R. A. Cox (2008), Sea salt aerosol production and bromine release: Role of snow on sea ice, *Geophys. Res. Lett.*, *35*, L16815, doi:10.1029/2008GL034536.
- Yang, X., J. A. Pyle, R. A. Cox, N. Theys, and M. Van Roozendael (2010), Snow-sourced bromine and its implications for polar tropospheric ozone, *Atmos. Chem. Phys.*, *10*, 7763–7773, doi:10.5194/acp-10-7763-2010.